Collagen and Leather

RESEARCH

Open Access

Improving the crosslinking of collagen casing and glutaraldehyde by facilitating the formation of conjugate structure via pH

Zhe Yu[1,2], Jingmin Wu[3], Ting Zhang[1], Chi Chen[1], Yun Ma[1], Hongxiang Liu[4,5], Bor-Sen Chiou[6], Fei Liu[1,2*] and Jian Li[7*]

Abstract

Glutaraldehyde (GTA) crosslinking is commonly used to improve the thermal stability and mechanical strength of collagen casings. The aim of this research was to determine the optimal pH of the crosslinking between GTA and collagen as well as the crosslinking mechanisms. The weakly alkaline environment could facilitate the generation of GTA polymerization through the rapid generation of -C=C-C=O and -N=C-C=C- conjugated structures, and enhance the crosslinking reaction of GTA polymers with collagen amino groups. In the pH range of 8–10, the fibril diameter and d-space value declined significantly in the self-assembled collagen fibril-GTA system. Meanwhile, collagen casing films crosslinked with GTA in weakly alkaline conditions exhibited higher mechanical strength and thermal stability. These results suggest that the crosslinking of collagen casings and GTA can be improved by adjusting the pH. Possible crosslinking mechanisms related to the formation of conjugated long chains have also been proposed. This study could provide guidance on the appropriate use of GTA in the production process of collagen casings.

Keywords Glutaraldehyde, Collagen casings, Crosslinking, pH, Conjugate structure

*Correspondence:
Fei Liu
feiliu@jiangnan.edu.cn
Jian Li
jian.li@jiangnan.edu.cn
Full list of author information is available at the end of the article

Graphical Abstract

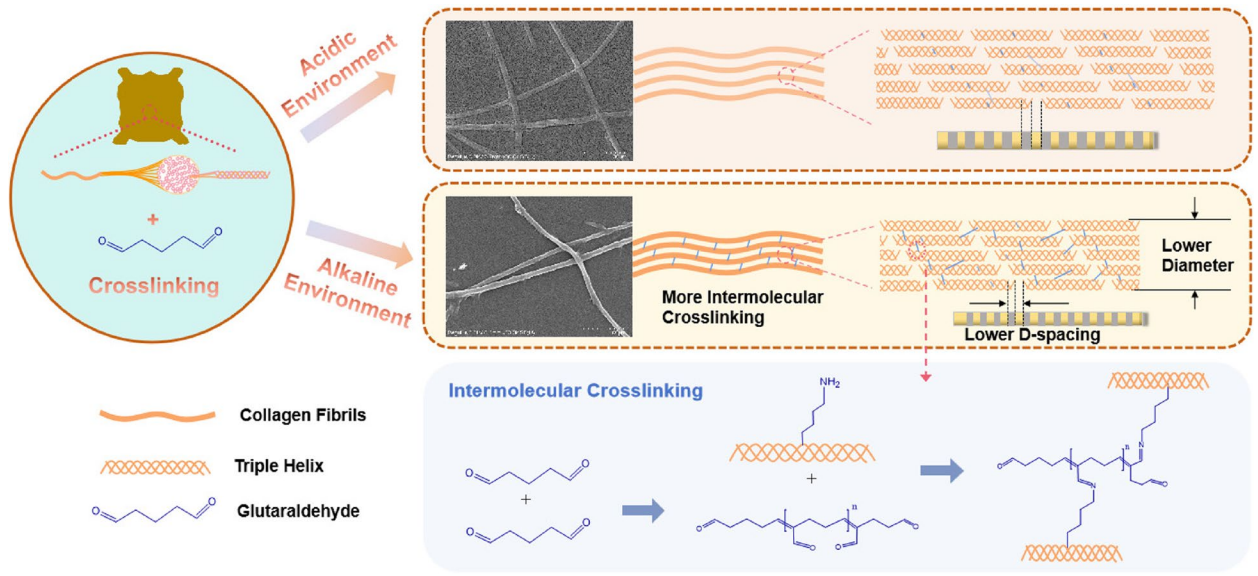

1 Introduction

Collagen-based materials display great potential in various fields such as food engineering [1], biochemistry [2], tissue engineering [3, 4] and smart materials area [5]. Glutaraldehyde (GTA) is an effective collagen crosslinking agent [6, 7]. GTA or its polymers can react with several functional groups in proteins, such as ε-amino groups, N-terminal amino groups of peptide chains, primary amines, imines, amides and hydroxyl groups [8]. It has been used to improve the mechanical properties [9], thermal stability [9, 10] and hydrophobicity [11] of collagen-based materials. Particularly, GTA has been approved for use in collagen casing by FDA for improving mechanical strength and thermal stability [12].

Early researchers believed that the GTA crosslinking reaction occurred to form a Shiff base between GTA and a free amino group [13]. However, more recent studies had found that the reactions and crosslinking effects are diverse [14, 15]. For instance, the reactivities of ε-amino groups, N-terminal amino group and primary amines with GTA are different, which cause GTA to have different reactions with proteins containing various amino acids. For example, GTA had shown higher reactivity with lysine [8, 16]. GTA mainly crosslinks with lysine residues in collagen [17, 18], and there are as many as 12 possible reaction mechanisms reported in literature [7]. Moreover, GTA concentration, crosslinking time [10, 17], temperature and pH value [15, 19] also affected the crosslinking reaction.

Previous studies had shown that pH had a large effect on the reaction between GTA and collagen or gelatin [20, 21]. Firstly, the form of GTA in aqueous solution is affected by pH, with GTA changing from monomer to polymer for an increase in pH [14, 22]. Secondly, pH affects the degree of collagen swelling and the integrity of the triple helix structure [23]. Finally, pH can also affect the charge on amino acid residues. A previous study found that amino protonation of lysine residue affected the crosslinking reaction [24]. Moreover, Schiff bases become unstable at low pH [25] and this can affect the crosslinking reaction. In the production process of collagen casings, the pH value varies greatly depending on the process steps. It is necessary to investigate the optimum pH and reaction mechanism of the crosslinking reaction between GTA and collagen to determine the GTA adding approach.

There are still questions about the optimal pH for crosslinking between GTA and collagen. A previous study found that the optimal pH for GTA crosslinked gelatin film was around 4.5 [26]. It has been found that the encapsulation efficiency of gelatin-GTA microcapsules was higher under acidic conditions [27]. Another study on collagen crosslinked with GTA at various pH values showed that collagen fibers changed from unordered to more ordered structures at a pH of 10 [18]. For other proteins, such as soy protein, GTA had been shown to be a better crosslinker under weak alkaline conditions [28, 29].

GTA also exists in several different molecular forms in aqueous solution, depending on solution conditions such as pH, concentration and temperature. Thirteen possible forms of GTA had been reported in literature, including free aldehydes, cyclic hemiacetal, cyclic hemiacetal oligomers and various hydroxyaldehyde polymers. Various reaction pathways were reported between GTA and protein based on different forms of GTA [14]. Early studies used ultraviolet spectroscopy and light scattering methods to analyze the existing forms of GTA in aqueous solution, but these methods were not sufficient to discriminate between different forms [30, 31]. Zuo et al. [32] found strong fluorescence of GTA in solution and used it to determine the molecular structure of GTA. Therefore, ultraviolet absorption combined with fluorescence emission could be used to determine the GTA forms and crosslinking mechanism. Previous studies have simulated the reaction between GTA and collagen at different pH values and proposed some reaction mechanisms [14, 24]. However, these mechanisms lack validation.

Due to the complexity of collagen-GTA crosslinking and the lack of relevant research, there are several issues that need to be addressed. For instance, studies have primarily focused on macroscopic characteristics, with limited observations of collagen fiber visualization and an incomplete understanding of collagen molecular mechanisms. In this study, we investigated the crosslinking of collagen casing films as well as single collagen fibers with GTA at different pH conditions to investigate the optimal pH. Meanwhile, existence forms of GTA and the reaction products of GTA with amino groups at different pH were further investigated to determine the crosslinking mechanism.

2 Materials and methods

2.1 Materials

Bovine corium was obtained from Beijing Qiushi Agriculture Development Co., Ltd. (Beijing, China). Pepsin was obtained from Sigma-Aldrich (Shanghai, China) and N-amylamine was obtained from Anpel (Shanghai, China). GTA (25% aqueous solution), phosphate buffered saline (PBS), acetic acid, hydrochloride and sodium hydroxide were obtained from Sinopharm (Shanghai, China). Tris-Glycine-SDS buffer solution, Coomassie Blue (G-250), acrylamide, timethylol aminomethane buffer, sodium dodecyl sulfate (SDS), ammonium persulfate, tetramethylethylenediamine, monopotassium phosphate, disodium hydrogen phosphate and potassium chloride were obtained from J&K scientific (Shanghai, China). The 10–250 KDa markers were obtained from Biocomma (Shengzhen, China).

2.2 Collagen film preparation and characterization

Collagen was extracted from dermal bovine tissue and pressed into films according to previous studies [33, 34]. After neutralization with ammonia, films were subsequently crosslinked in GTA solutions (50 ppm, w/w) for 30 min at pH of 3.0, 4.5, 6.0, 7.0, 8.5 and 10.0 (designated as GTA group). Samples without GTA crosslinking at various pH values were designated as the control group. Then films were soaked in plasticizer solution (4% w/w glycerol solution) for 25 min and removed and dried in a 30 °C oven for 24 h. The dried sample was equilibrated in a constant temperature and humidity tank (25 °C, 52% relative humidity (RH)) for 72 h before tests.

Heating shrinkage rate, tensile strength (wet and boiled 1 min) and swelling ratio were determined following the previous reported methods [34].

Fluorescence images of cross-linked collagen casings were acquired using a fluorescence microscope (80i, Nikon Co., Ltd., Japan). Collagen films without crosslinking at the same pH conditions were used as control and adjusted to be non-fluorescent.

2.3 Analysis of existing GTA forms in PBS solution

2.3.1 Ultraviolet (UV) spectrometry

PBS solutions (0.2 mol/L) were prepared with pH varying from 4 to 10 (4, 5, 6, 7, 8, 9 and 10). GTA was introduced to each PBS solution with the final GTA concentration reaching 50 mg/L. Sample solutions were incubated for 30 min, 12 h, 24 h and 48 h and then transferred into a quartz cell in a UV spectrophotometer (UV2450, Shimadzu, Kyoto, Japan). Samples were then measured from 200 to 400 nm. Samples were labelled as G-pH value-time.

2.3.2 Fluorescence emission spectrometry

Fluorescence measurements were determined according to the method described by Zuo et al. [32], with slight modifications. The same GTA solutions used for UV spectroscopy (see Section 2.3.1) were also used for fluorescence spectroscopy. Analyses were performed via emission spectrometry (F-7000, Hitachi, Tokyo, Japan) from 430 to 600 nm. The excitation wavelength was 410 nm. Parameter values of excitation band and emission band were all 10 nm. The data were collected at 0.5 nm intervals. Samples were labelled as G-pH value-time.

2.4 Analysis of existing GTA forms in n-amylamine - GTA model system

PBS solutions (0.2 mol/L) were first prepared with pH varying from 4 to 10 (4, 5, 6, 7, 8, 9 and 10). GTA (50 mg/L) and n-amylamine (0.1 mmol/L) were then

added to the solutions. UV spectrometry and fluorescence emission spectrometry were used to characterize the solutions based on methods described in Sections 2.3.1 and 2.3.2. Samples were labelled as GN-pH values-time.

2.5 Collagen extraction

Collagen was extracted from bovine corium [35]. Bovine corium cubes were thawed at ambient temperature and mixed with ice cubes at the ratio of 1:2.5 (corium cubes: ice). The sample was mixed using high-speed shearing (DFY-200C, Linda Machine, China) for 10 min. Then, 0.5 mol/L acetic acid (20 times corium pulp weight, w/w) and pepsin (2% of the corium pulp weight, w/w) were added to the bovine corium pulp. The final pH of the mixed solution was adjusted to 2.5 and the pulp was stirred at 4 ℃ for 24 h. The solution was centrifuged (10,000 r/min) at 4 ℃ for 20 min. The supernatant was then precipitated by adding NaCl to 2.0 mol / L. The sample was centrifuged (10,000 r/min) again at 4 ℃ for 20 min and the precipitate was collected. Next, the precipitate was dissolved in 0.5 mol/L acetic acid and the desalting purification procedure was repeated one more time. The resulting collagen solution was dialyzed by using an 8000–14000 MW dialysis bag at 4 ℃ for 48 h. The deionized water was replaced every 6 h. The dialyzed collagen solution was lyophilized and stored at 4 ℃.

2.6 Structure analysis of extracted collagen

2.6.1 Attenuated total reflectance-Fourier transform infrared spectroscopy (ATR-FTIR)

The chemical properties of lyophilized collagen were characterized by using a FTIR spectrometer (Nicolet IS 50, Thermo Electron, USA) in ATR mode. Background scanning was applied prior to each test. Each spectrum contained 32 scans from 800 to 4000 cm^{-1} at a resolution of 4 cm^{-1}.

2.6.2 Sodium dodecyl sulfate polyacrylamide gel electrophoresis (SDS-PAGE)

SDS-PAGE was performed according to the method of Sun [36]. Lyophilized collagen was first dissolved in 0.1 mol/L of acetic acid to make a 1 mg/mL solution, diluted and mixed with Tris-Glycine-SDS buffer solution at a ratio of 3:1 collagen solution to buffer solution. The mixture was boiled for 5 min and then centrifuged at 10,000 rpm for 5 min. The supernatant (10 μL) was loaded onto the gel. A 10% resolving gel and 4% stacking gel were used in the tests. The ingredients are shown in Table 1. Gel electrophoresis (Mini Protean Tetra, bio-rad, USA) was then used to separate the proteins. The polyacrylamide gel was dyed with Coomassie Blue (G-250) for 2 h and rinsed with water. A gel imaging system (ChemiDoc XRS+, bio-rad, USA) and molecular weight markers (10–250 KDa) were used to determine the molecular weights of the proteins.

Table 1 Composition of resolving and stacking gel

Component	10% resolving gel (mL)	4% stacking gel (mL)
Deionized water	4	3
Acrylamide (30%, 29:1)	3.3	0.67
1 mol/L Tris (pH 6.8)	-	1.25
1.5 mol/L Tris (pH 8.8)	2.5	-
10% SDS	0.1	0.05
10% ammonium persulfate	0.1	0.05
Tetramethylethylenediamine	0.004	0.005

2.7 Analysis of collagen self-assembly

The self-assembly of collagen was determined according to the method of Yan et al. [37]. The lyophilized collagen was first dissolved in 0.5 mol/L acetic acid solution (5 mg/mL collagen) and intermittently stirred at 4℃ for 30 min. The sample was centrifuged (10,000 r/min) at 4℃ for 20 min to obtain a supernatant solution. The concentration of collagen solution was diluted to 1 mg/mL with PBS solution (10 mmol/L of monopotassium phosphate, 30 mmol/L of disodium hydrogen phosphate and 20 mmol/L of potassium chloride) and 1 mol/L of disodium hydrogen phosphate solution at a volume ratio of 2:7:1 (collagen solution: PBS solution: disodium hydrogen phosphate solution). The beaker with the resulting mixture was placed into an ice slurry to keep the collagen stable. The start of collagen self-assembly was triggered by putting the mixture solution into a 37℃ thermostatic water bath. 2 mL of collagen solutions were taken out at different times and analyzed using the ultraviolet spectrophotometer at a wavelength of 313 nm (Fig. S1).

2.8 Collagen fibril crosslinking with GTA

The self-assembled collagen fibril solution (2 mL) was diluted to 18 mL using 50 mmol/L PBS solutions (pH of 4–10). The pH of the mixture was adjusted back to the original pH of the PBS solution by using hydrochloride acid and sodium hydroxide. Crosslinking started when GTA (50 mg/L) was added to the solutions. The samples were tested after crosslinking for 30 min, 12 h, 24 h and 48 h. Samples with GTA crosslinking were denoted as GTA-pH value. Samples without GTA crosslinking were denoted as con-pH value.

2.9 Structure analysis of collagen fibril

2.9.1 Atomic force microscopy (AFM)

Drops of the solution containing diluted self-assembled collagen fibrils were placed on a glass slide. A rubber gasket was used to secure and trap the liquid sample. An AFM (Dimension FastScan, Bruker, Germany) with a surface morphology probe was used to examine the sample at 25℃ with the setting of mapping mode and 3×3 μm^2 scan size.

2.9.2 Field emission scanning electron microscopy (FESEM)

An aliquot (10 µL) of the collagen fibril solution was placed onto a silicon wafer. The sample was dried at 30℃ for 24 h in a water-proof constant temperature incubator (GHP-9160D, Shanghai, China). The sample was rinsed with deionized water before the drying process. Next, the dried silicon wafer containing the sample was sputter coated with Au/Pd. An FESEM (SU8100, Hitachi, Japan) was used to examine the morphology of the collagen fibrils under 3 kV accelerating voltage. Image J was used for photo editing.

2.9.3 Small-angle X-ray scattering (SAXS)

SAXS (SAXSpoint2.0, Anton Paar, Austria) was used to determine the structure of the collagen fibrils. The voltage was 50 kV, the current was 40 mA and the λ was 0.154 nm. The measure distance was set at 600 mm and data were collected for 10 min. Each sample was tested in triplicate and data were processed using Fit2D and SGI. The D-spacing can be calculated by equation $D=2\pi/q$. Value of q is the distance between intensity peaks [38, 39].

3 Results

3.1 Crosslinking effects of GTA with collagen films at different pH values

Collagen fibrils shrink under hydrothermal conditions [40] and the shrinkage temperature and shrinkage rate of collagen films can macroscopically reflect the degree of crosslinking [34]. With no GTA crosslinking (Fig. 1a), the shrinkage rates were compared at various pH values. The shrinkage rates reached a plateau at around 65 ℃ and did not increase with an increase in temperature. However, the GTA crosslinked samples showed a different behavior (Fig. 1b). Most samples showed a significantly lower shrinkage rate at around 65 ℃ compared to the non-crosslinked samples. The shrinkage rate gradually decreased in value at higher temperatures without showing a plateau temperature. The samples with a pH of 8–10 showed larger decreases in shrinkage rates compared with the others. The shrinkage rate also decreased in the pH 4 samples. That could be related to the destruction of collagen fiber structure. It has been demonstrated in the literature that collagen is less thermally stable and more susceptible to thermal denaturation at lower pH values [41]. Similarly, at the pH range of 8–10, the crosslinked

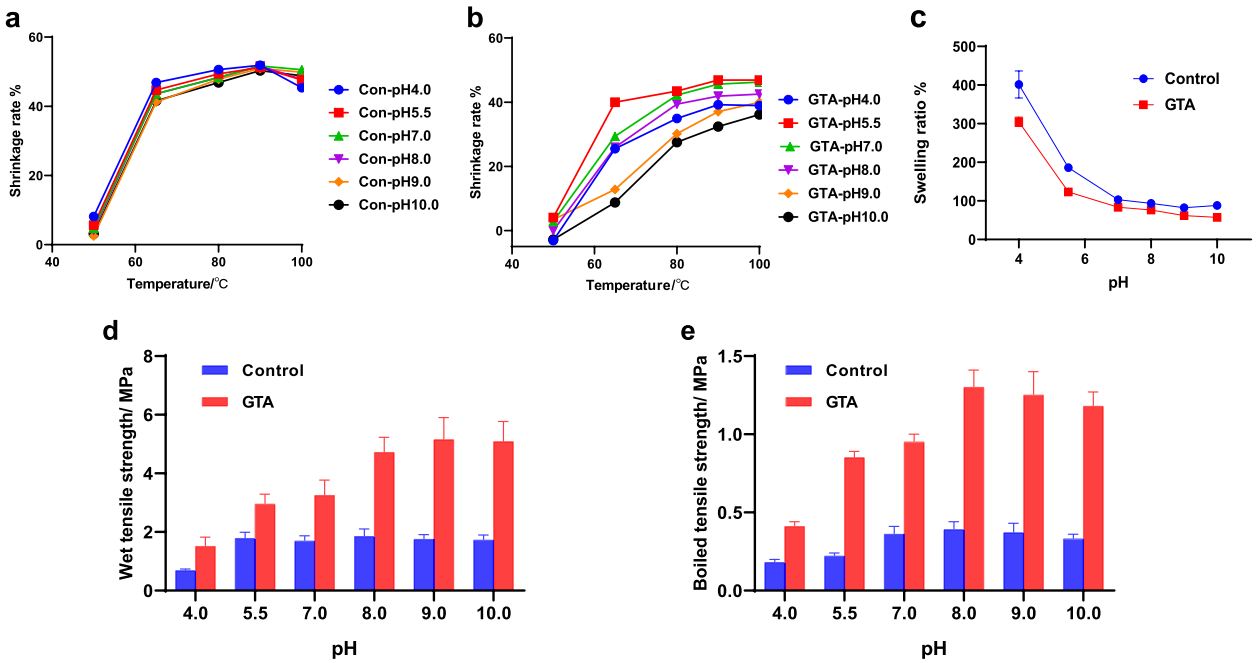

Fig. 1 Properties of GTA crosslinked and non-crosslinked collagen films at different pH values: **a** shrinkage rate of non-crosslinked collagen films, **b** shrinkage rate of GTA crosslinked collagen films and **c** swelling ratio, **d** wet tensile strength, **e** boiled tensile strength

collagen casing films achieved greater increases in mechanical properties (Fig. 1d, e). These indicated that the samples at a pH of 8–10 had greater crosslinking.

The swelling ratio is water absorption rate of the collagen casing film after boiling, which reflects the water resistance of collagen [34]. Figure 1c shows the swelling ratios of collagen films with and without GTA crosslinking at different pH values. At pH 4, the absolute value of the swelling rate was higher, probably due to the isoelectric point of collagen being further away from 4. Studies have shown that the isoelectric point of collagen I with complete structure is between 6.7–7.9 [42, 43]. For crosslinked samples, the GTA reacted with hydrophilic amino groups that caused a decrease in the swelling ratios for all samples. This indicated that crosslinking occurred at all pH values. However, both the shrinking rate and tensile strength results indicated that more crosslinking occurred under weakly alkaline conditions.

3.2 Crosslinking effects of GTA with collagen fibrils at different pH values

The effect of pH on the crosslinking of single collagen fibrils with GTA was further observed. Collagen with high integrity triple helix structures can self-assemble in vitro, unlike gelatin and hydrolyzed collagen. Figure S1 shows the line graph of the dynamic self-assembly of collagen in vitro. Absorbance became stable after 80 min when incubated at 37℃, indicating the self-assembly process had been completed [44]. Complete collagen triple helix structure extracted from bovine dermis is shown in Fig. 2a. The peak intensity ratio of A_{1240}/A_{1450} is associated with the integrity of the triple helix structure [45]. The A_{1240}/A_{1450} ratio for the extracted collagen was determined to be 0.98, which indicated high integrity of the collagen triple helix structure [46] and could be used for the crosslinking experiments.

The SEM micrographs of non-crosslinked and GTA crosslinked collagen fibrils are shown in Fig. 2b and c, respectively. In the non-crosslinked group, the sample at pH of 4 contained several small fibril sections and relatively few fully formed fibrils. An increase in pH led to the formation of fibrils with higher integrity and the appearance of typical fibril structures. In the crosslinking group, after GTA treatment for 30 min, the collagen fibrils became more stereoscopic, which may be due to the increased rigidity of the fibers after crosslinking. In addition, Table 2 shows the diameters of the collagen fibrils. There was no radial shrinkage of collagen fibers after GTA immersion at pH 4–5. Collagen fibrils shrunk 22.0–33.3% in diameter after treatment at pH 6–7. As for pH 8–10, however, the collagen fiber diameter shrinkage reached 37.6–38.0%. This may indicate that the crosslinking between collagen and GTA is more reactive at pH 8–10, which is consistent with the appearance of the collagen casing film.

3.3 Collagen fibril SAXS analysis

SAXS analysis can be used to investigate structures ranging from 1–100 nm and be used to help understand hydration, orientation and D-periodicity of collagen in the crosslinking process [38, 47]. The 2D SAXS diffraction images of GTA crosslinked and non-crosslinked samples are shown in Fig. 3, and the D-periodicity of each sample was calculated based on Fig. S2. No clear diffraction rings could be observed in the sample at a pH of 4 since the collagen fibrils could have swollen too much and disrupted the crystal structure. The D-periodicity of collagen fibrils varied between 63.69 and 65.82 nm for the non-crosslinked group. These results were consistent with the d-spacing results found by Sizeland et al. during leather preparation [48].

The d-space values of cross-linked collagen samples at pH 5–7 were greater than 63.69 nm. In comparison, samples with a pH greater than 8 had d-space values lower than 63.69 nm, indicating axial packing had occurred in the fibrils. Also, the diffraction peak intensities for crosslinked samples with a pH greater than 8 were significantly lower than those of the non-crosslinked samples. This might be due to the conjugated double bonds formed by alkaline crosslinking that interfered with the electron density cloud between collagen molecules. Although the crosslinked samples had lower peak intensity than the non-crosslinked samples, their diffraction peaks corresponding to the collagen d-spacing can still be observed in the diffraction curves (Fig. S2).

3.4 Existing GTA forms in solutions with different pH values

Possible existing forms of GTA in solution include monomer, hemiacetal, oligomer and polymer. GTA hydroxy aldehyde polymer has a strong ultraviolet absorption [22, 49], with the maximum absorption wavelength of 235 nm. This corresponds to the $\pi \rightarrow \pi^*$ transition of a conjugated ethylene double bond [50, 51]. The molar absorption coefficient of GTA free monomer is about 1,000 times smaller than that of hydroxyaldehyde polymer, so there is only weak absorption at 280 nm [22]. The UV absorption of the acetal and hemiacetal forms of GTA have not been reported in literature. Therefore, UV absorption can be used to characterize the changes in amounts of hydroxy aldehyde polymer with pH.

Figure 4 shows the ultraviolet absorption spectra of GTA solutions at different pH values over 48 h. Within 30 min, each GTA solution showed a characteristic absorption peak at 235 nm, which was due to the presence of unsaturated polymer impurities. The

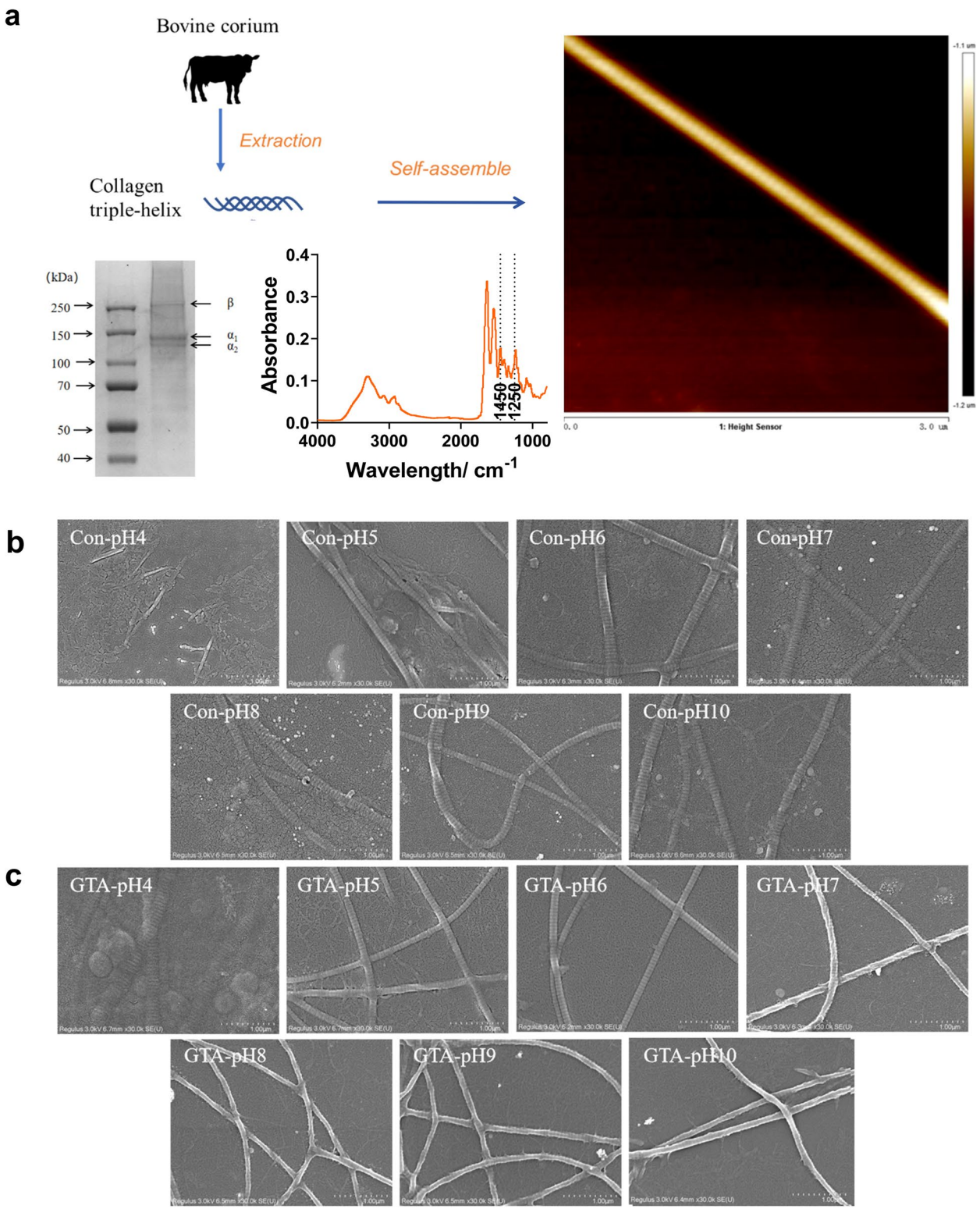

Fig. 2 **a** Extracted collagen structure and its self-assembly. Collagen fibers microstructures: **b** non-crosslinking group and **c** crosslinking group

Table 2 Diameters of collagen fibrils in non-crosslinking group and GTA-crosslinking group

pH	Diameter (μm)	
	Non-crosslinking	GTA-crosslinking
pH4	0.204 ± 0.024^{f}	0.216 ± 0.017^{f}
pH5	0.143 ± 0.015^{c}	0.151 ± 0.041^{cd}
pH6	0.174 ± 0.019^{e}	0.137 ± 0.012^{c}
pH7	0.177 ± 0.015^{e}	0.118 ± 0.025^{b}
pH8	0.176 ± 0.034^{e}	0.109 ± 0.009^{ab}
pH9	0.164 ± 0.024^{de}	0.102 ± 0.011^{a}
pH10	0.162 ± 0.018^{de}	0.101 ± 0.014^{a}

Different superscripts indicate significant differences ($P < 0.05$)

GTA solution with pH of 4 showed the most stable spectrum over time, with the absorption peaks showing no significant changes. In acidic and neutral solutions (pH of 5–7), the unsaturated polymer absorption peak (235 nm) slightly increased with time. In alkaline solutions, the absorbance peak at 235 nm significantly increased in value with time. This indicated that the GTA molecules may undergo aldol condensation reactions under alkaline conditions to form an unsaturated polymer with the structure of -C = C-C = O. After 48 h (Fig. 4d), the absorption peak of the sample at a pH of 10 was significantly blue shifted, indicating that the degree of conjugation increased over time.

Molecules with conjugated π-π structure normally provide strong fluorescence signals. The GTA monomer is a 5-carbon dialdehyde that does not fluoresce since the energy required for an $n \rightarrow \sigma^*$ electronic transition is high. Nevertheless, polymerized GTA forms have conjugate structures of C = C and C = O, enabling electronic transitions of $\pi \rightarrow \pi^*$ and $n \rightarrow \pi^*$ [32]. Strong fluorescence signals can be detected in polymerized GTA with extended conjugate structures.

Figure 5 presents fluorescence emission spectra of GTA solutions with different pH values over 48 h. A peak at 478 nm was detected in all GTA solutions at short incubation time. This peak might be due to small amounts of polymerized GTA in the samples. An increase in peak intensity only occurred at longer times for the GTA solution with a pH of 10. This might be due to the limited GTA polymerization occurring under acid/neutral conditions.

From the ultraviolet absorption and fluorescence results, alkaline conditions are more conducive to the polymerization of GTA and the formation of conjugated structures than neutral or acidic conditions.

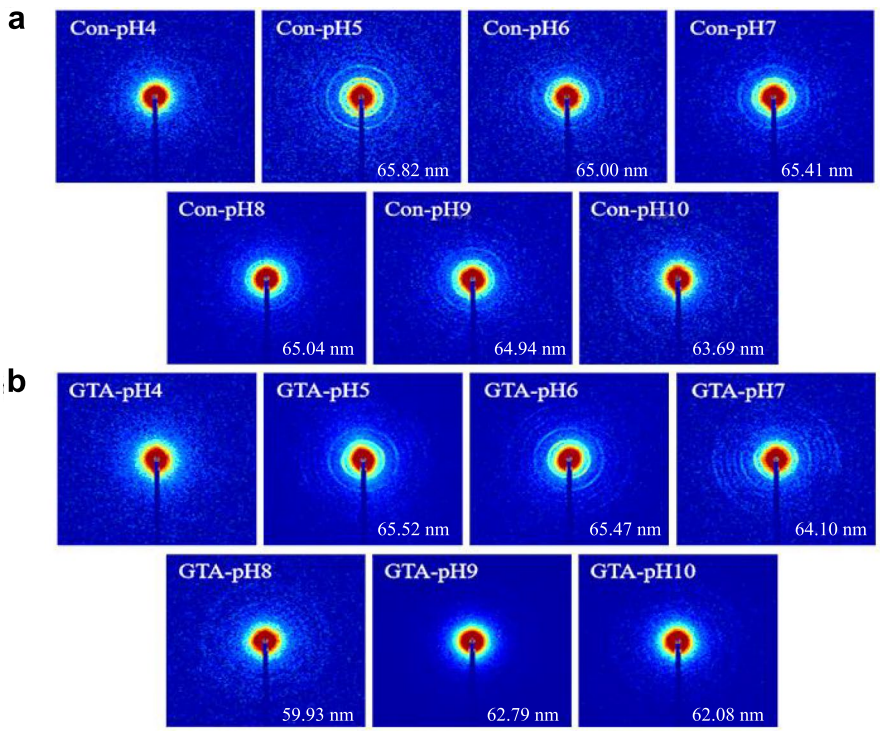

Fig. 3 SAXS diffraction patterns of collagen fibrils: **a** non-crosslinking group and **b** crosslinking group

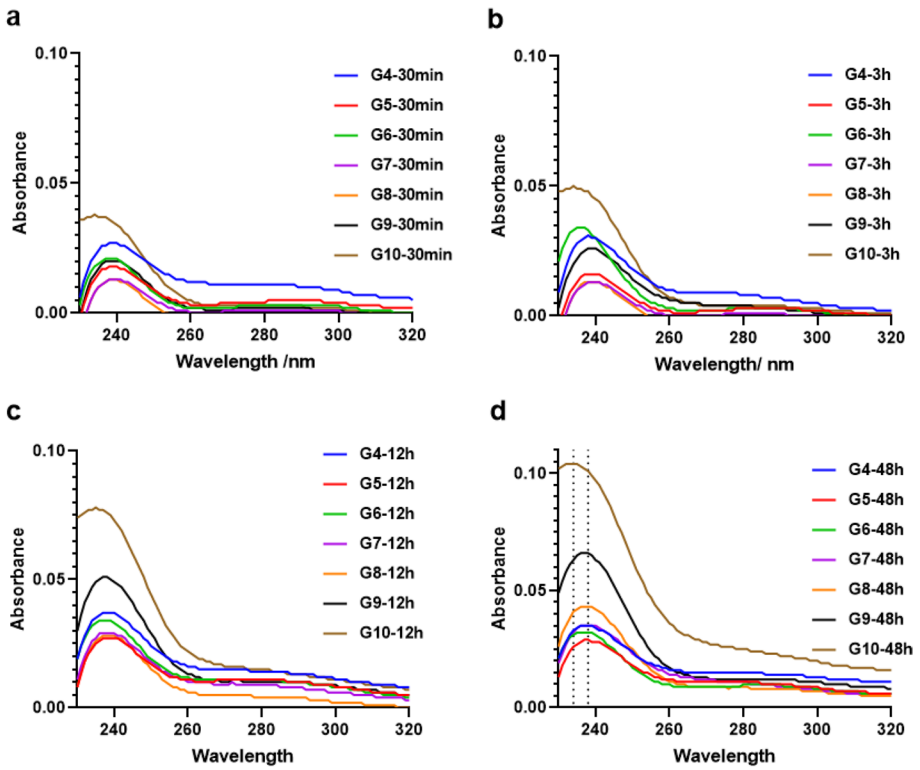

Fig. 4 UV spectra of GTA solutions with different pH values (pH of 4–10) and incubation time: **a** 30 min, **b** 3 h, **c** 12 h and **d** 48 h

3.5 Simulated crosslinking in model n-amylamine-GTA system

From previous studies, it is known that GTA and its polymers may react preferentially with the amino groups in the lysine residues in collagen [8, 16–18]. However, since collagen is an insoluble macromolecule, characterizing the chemical reaction pathways from the molecular level faces difficulties. In the present study, we intend to use soluble n-amylamine to explore the possible pathways of GTA reaction with collagen tentatively.

N-amylamine was added to the GTA solutions to determine which GTA forms existed in a crosslinking system. Figure 6 shows the ultraviolet and fluorescence spectrometry results of the model systems with different pH values and incubation times. The GTA and n-amylamine sample with a pH of 10 showed a rapid increase in the absorbance peak at 235 nm after 30 min. The pH of the solution was the crucial factor in enhancing the rapid generation of conjugated structures. At longer incubation times, all samples showed an increase in peak intensity, although the largest increases occurred under higher pH conditions (Fig. 6a). The blue-shift of the peaks for samples with pH values above 8 suggested an increase in the degree of polymerization. The samples containing n-amylamine showed larger increases in the peak intensity at 235 nm compared to the samples without n-amylamine. For instance, the GTA-n-amylamine sample at a pH of 10 had a peak intensity after 30 min that was double that of the GTA sample without n-amylamine (Fig. 4a). These results were consistent with a previous study, which found that the GTA polymerized more readily with other GTA molecules when the sample included the formation of Schiff bases from the reaction between GTA and amino groups [30]. Similar results were obtained in the lysine-GTA model (Figure S3).

The fluorescence emission spectrometry results were similar to those from UV spectrometry and indicated the formation of C=C and C=O conjugate structures. In addition, a weak peak near 560 nm appeared when the crosslinking time was over 12 h (Fig. 6b). This has not been reported in previous studies. This peak did not appear in the GTA solutions without n-amylamine, and it might be related to the -N=C-C=C-conjugate double bond generated by one of the GTA and amino group reactions.

These results indicated that both a high pH and the presence of amino groups are important elements for inducing conjugate polymerization in the GTA-n-amylamine system. The possible conjugate structures should include -N=C-C=C- and -C=C-C=O. Hence, we proposed a possible crosslinking mechanism of GTA with amino groups under weak alkaline conditions in Fig. 6c.

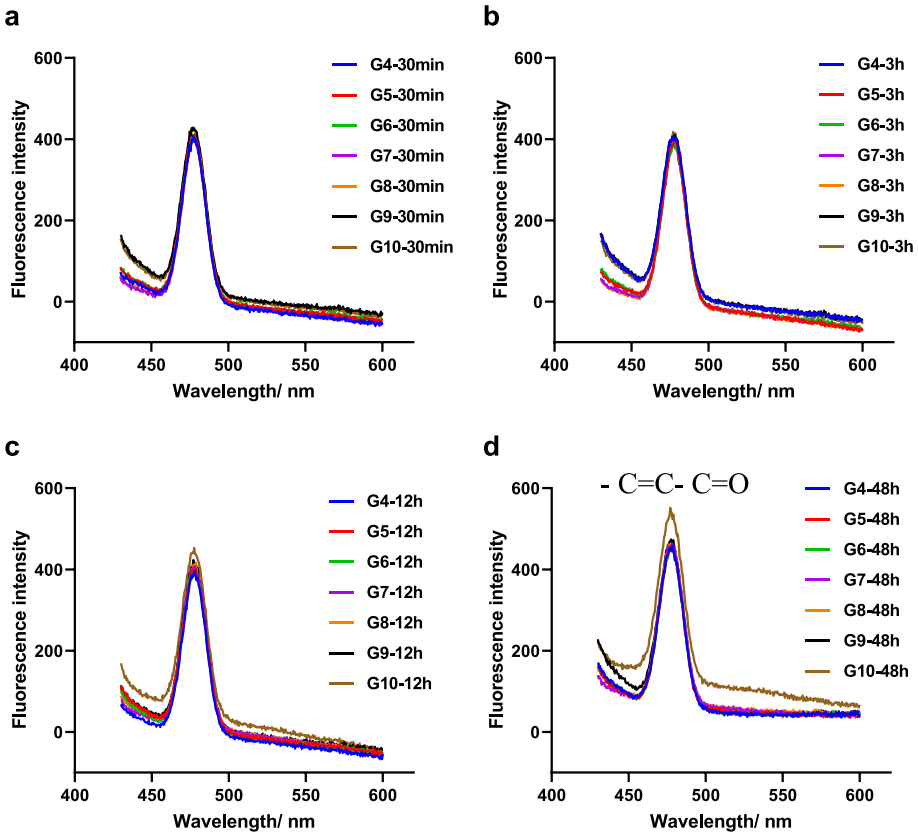

Fig. 5 Florescence spectra of GTA solutions with different pH values (pH 4–10) and incubating times: **a** 30 min, **b** 3 h, **c** 12 h and **d** 48 h

3.6 Fluorescence microscopic observation of collagen casing films

Figure 7a shows the fluorescence microscopy images of collagen casing films after crosslinking at different pH. No obvious auto-fluorescence was found at pH 4. The fluorescence intensity gradually increased with the increase of pH. It can be speculated that -N=C-C=C- and -C=C-C=O conjugated double bonds are produced due to polymerization of GTA and reaction with collagen.

To summarize the results in this paper, the GTA hydroxyl aldehyde condensation reaction and the collagen crosslinking are simultaneous and mutually reinforcing when crosslinking under weakly alkaline conditions. It can be hypothesized that GTA polymers play an important role in the crosslinking reaction of collagen. Due to the long molecular chain of the polymer, intermolecular crosslinking can be generated thereby causing axial and radial stacking of collagen fibrils, enhancing the crosslinking effect. Figure 7b illustrates the crosslinking reaction of collagen fibrils with GTA polymers under weak alkaline conditions. These may be the reasons for the larger increase in mechanical strength and lower shrinkage of crosslinked collagen casings at pH 8–10 (Fig. 1). It should be pointed out that Fig. 7b only provides one crosslinking reaction pathway under pH 8–10 conditions, and this pathway may occur rarely at pH 4.0, but it does not mean that there are no other mechanisms. Moreover, even the reaction between lysine residues and GTA polymers possessing long molecular chains, the active sites are not exclusive, and some other possible reaction pathways are shown in Fig S4.

4 Conclusion

In this work, we determined the optimum pH and the possible mechanism of pH-induced crosslinking changes between GTA and collagen casing films. In the pH range of 8–10, the crosslinked collagen casing films achieved greater increases in mechanical properties. Meanwhile, the shrinkage rate of collagen films crosslinked under weakly alkaline conditions was lower than that of films under acidic conditions, indicating greater degrees of crosslinking. Also, GTA crosslinked collagen showed decreases in fibril diameters and d-space values in weakly alkaline conditions. UV and fluorescence spectrometry results suggested that GTA polymers with -C=C-C=O conjugated structures were easily generated in GTA (50 ppm) solution at pH values greater than 7. The presence of n-amylamine also could lead to the generation

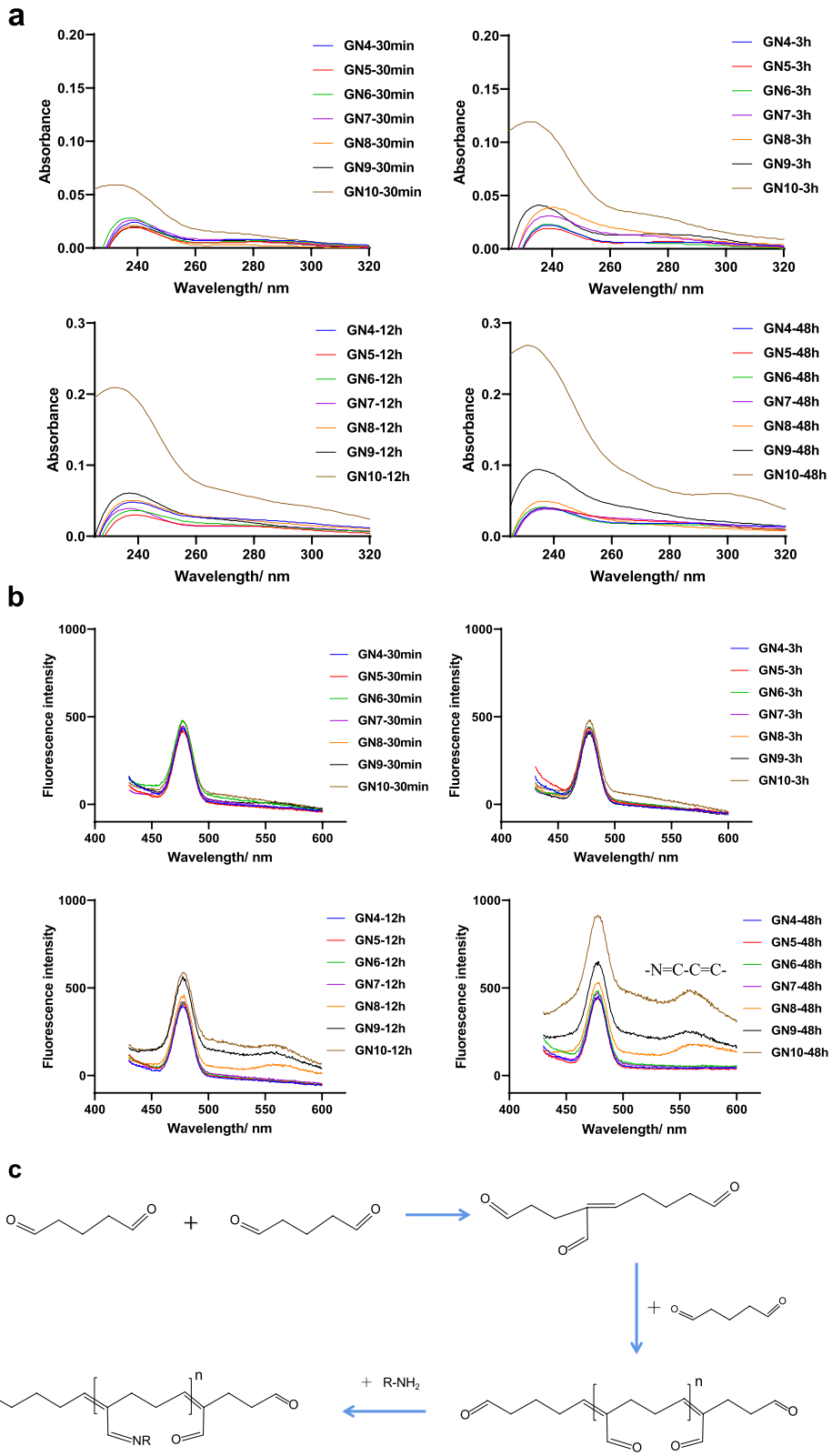

Fig. 6 UV spectra (Wavelength-Absorbance) and fluorescence spectra (Wavelength-Intensity) of n-amylamine-GTA model crosslinking solution with different pH values: **a** UV spectra and **b** fluorescence spectra. **c** Possible crosslinking mechanism of GTA and amino group under weak alkaline conditions

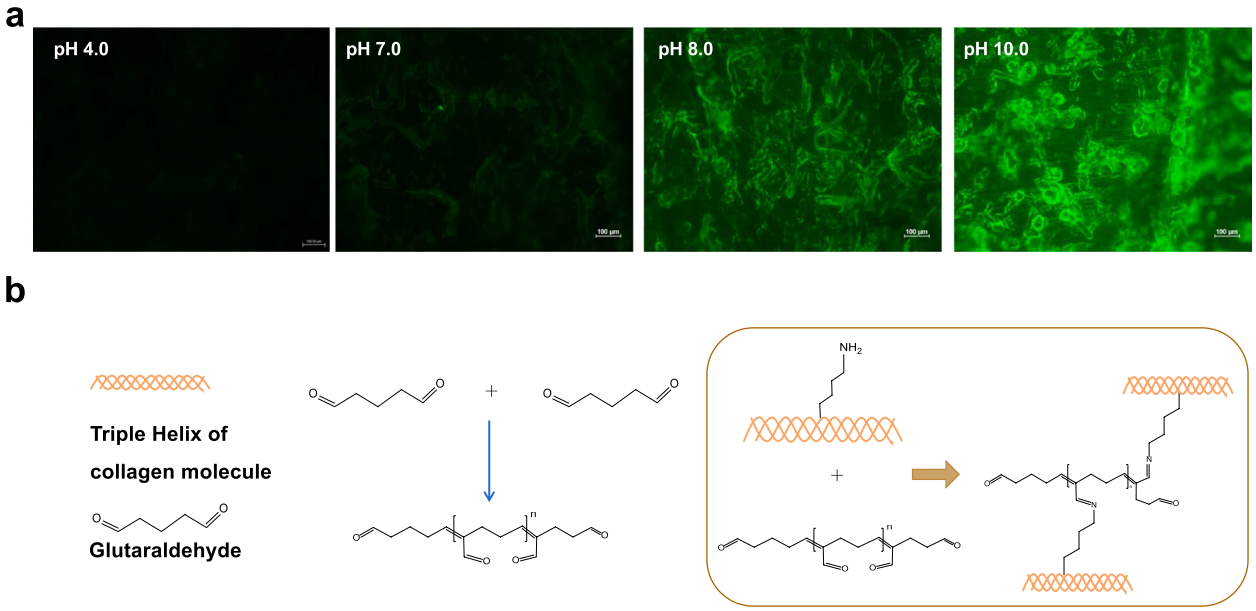

Fig. 7 **a** Fluorescence micrographs of collagen casing films cross-linked with GTA at different pH values. **b** Possible crosslinking mechanism of GTA and collagen under weak alkaline conditions

of more conjugate structures. The fluorescence results of GTA-n-amylamine samples at a pH greater than 7 indicated the presence of two conjugated structures at 478 nm and 560 nm, which may be corresponded to the GTA polymer (-C=C-C=O) and the reaction with amino groups (-N=C-C=C-), respectively. Similar fluorescence enhancement phenomenon was found in the collagen casing films which was crosslinked at pH > 7 condition, indicating the conjugated compounds in the films. Based on these results, we proposed a possible crosslinking mechanism under weakly alkaline conditions. GTA could generate conjugated polymers with long molecular chains and react with intermolecular amino groups, causing densification of collagen fibers and increasing the degree of crosslinking of collagen casing films, resulting in higher thermal stability and mechanical strength.

Supplementary Information

The online version contains supplementary material available at https://doi.org/10.1186/s42825-024-00172-8.

Supplementary Material 1.

Acknowledgements
The authors would like to thank Beijing Qiushi Collagen Casings Co., Ltd. for the cowhide material providing.

Authors' contributions
Zhe Yu: Investigation, Methodology, Software, Validation, Writing, Reviewing. Jingmin Wu: Methodology, Writing. Ting Zhang: Methodology, Conceptualization, Data curation, Validation. Chi Chen, Yun Ma, Hongxiang Liu: Methodology, Validation. Bor-Sen Chiou: Methodology, Writing- Reviewing and Editing. Fei Liu, Jian Li: Supervision, Investigation, Resources, Supervision, Project administration.

Funding
This research was supported by National Key R&D Program of China (2023YFF1104302), the Soft Science Research Project of Wuxi Science and Technology Association (KX-23-C042), and the program of "Collaborative Innovation Center of Food Safety and Quality Control in Jiangsu Province", China.

Availability of data and materials
Data will be made available on reasonable request.

Declarations

Ethics approval and consent to participate
Not applicable.

Consent for publication
Not applicable.

Competing interests
Bor-Sen Chiou serves as the deputy Editor-in-Chief of Collagen and Leather, and was not involved in the editorial review, or the decision to publish this article. All authors declare that there are no competing interests.

Author details
[1]State Key Laboratory of Food Science and Resources, Science Center for Future Foods, School of Food Science and Technology, International Joint Laboratory on Food Safety, Jiangnan University, Wuxi 214122, China. [2]Jiaxing Institute of Future Food, Jiaxing 314050, China. [3]Department of Food Technology, Food Safety and Health, Faculty of Bioscience Engineering, Ghent University, Coupure Links 653, Ghent 9000, Belgium. [4]Faculty of Biotechnology and Food Engineering, Technion - Israel Institute of Technology, Haifa 3200003, Israel. [5]Biotechnology and Food Engineering Program, Guangdong Technion - Israel Institute of Technology, Shantou 515063, China. [6]Western Regional Research Center, ARS, U.S. Department of Agriculture, Albany, CA 94710, USA. [7]Laboratory of Environmental Biotechnology, School of Environment and Ecology, Jiangnan University, Wuxi 214122, China.

Received: 10 March 2024 Revised: 17 June 2024 Accepted: 8 July 2024
Published online: 01 October 2024

References

1. Luo QY, Hossen MA, Zeng YB, Dai JW, Li SQ, Qin W, et al. Gelatin-based composite films and their application in food packaging: a review. J Food Eng. 2022;313:110762. https://doi.org/10.1016/j.jfoodeng.2021.110762. PubMed PMID: WOS:000693999800009.
2. Irastorza A, Zarandona I, Andonegi M, Guerrero P, de la Caba K. The versatility of collagen and chitosan: from food to biomedical applications. Food Hydrocoll. 2021;116:106633. https://doi.org/10.1016/j.foodhyd.2021.106633. PubMed PMID: WOS:000626462900001.
3. Chen H, Xue L, Gong G, Pan J, Wang X, Zhang Y, et al. Collagen-based materials in reproductive medicine and engineered reproductive tissues. J Leather Sci Eng. 2022;4:3. https://doi.org/10.1186/s42825-021-00075-y.
4. Rico-Llanos GA, Borrego-Gonzalez S, Moncayo-Donoso M, Becerra J, Visser R. Collagen type I biomaterials as scaffolds for bone tissue engineering. Polymers. 2021;13(4):20. https://doi.org/10.3390/polym13040599. PubMed PMID: WOS:000624253800001.
5. Han Y, Hu J, Sun G. Recent advances in skin collagen: functionality and non-medical applications. J Leather Sci Eng. 2021;3:4. https://doi.org/10.1186/s42825-020-00046-9.
6. Adamiak K, Sionkowska A. Current methods of collagen cross-linking: review. Int J Biol Macromol. 2020;161:550–60. https://doi.org/10.1016/j.ijbiomac.2020.06.075. PubMed PMID: WOS:000572333900009.
7. Damink LHHO, Dijkstra PJ, Luyn MJAV. Glutaraldehyde as a crosslinking agent for collagen-based biomaterials. J Mater Sci: Mater Med. 1995;6(8):460–72. https://doi.org/10.1007/bf00123371.
8. Hopwood D, Callen CR, McCabe M. The reactions between glutaraldehyde and various proteins. An investigation of their kinetics. Histochem J. 1970;2(2):137–50. https://doi.org/10.1007/bf01003541.
9. Tian Z, Shen L, Liu W, Li G. Construction of collagen gel with high viscoelasticity and thermal stability via combining cross-linking and dehydration. J Biomed Mater Res A. 2020;108(9):1934–43. https://doi.org/10.1002/jbm.a.36956.
10. Peng YY, Glattauer V, Ramshaw JAM. Stabilisation of collagen sponges by glutaraldehyde vapour crosslinking. Int J Biomater. 2017(1):8947823. https://doi.org/10.1155/2017/8947823.
11. Chen XF, Meng J, Xu HZ, Shinoda M, Kishimoto M, Sakurai S, et al. Fabrication and properties of electrospun collagen tubular scaffold crosslinked by physical and chemical treatments. Polymers. 2021;13(5):16. https://doi.org/10.3390/polym13050755. PubMed PMID: WOS:000628408000001.
12. FDA. Food additive status list. 2022. 2021. https://www.fda.gov/food/food-additives-petitions/food-additive-status-list.
13. Uragami T, Matsuda T, Okuno H, Miyata T. Structure of chemically modified chitosan membranes and their characteristics of permeation and separation of aqueous ethanol solutions. J Membr Sci. 1994;88(2–3):243–51. https://doi.org/10.1016/0376-7388(94)87010-1.
14. Migneault I, Dartiguenave C, Bertrand MJ, Waldron KC. Glutaraldehyde: behavior in aqueous solution, reaction with proteins, and application to enzyme crosslinking. Biotechniques. 2004;37(5):790–802. https://doi.org/10.1016/j.lfs.2005.04.043.
15. Lubig R, Kusch P, Röper K, Zahn H. On the mechanism of protein crosslinking with glutaraldehyde. Monatsh Chem. 1981;112(11):1313–23. https://doi.org/10.1007/bf00904683.
16. Wine Y, Cohen-Hadar N, Freeman A, Frolow F. Elucidation of the mechanism and end products of glutaraldehyde crosslinking reaction by X-ray structure analysis. Biotechnol Bioeng. 2007;98(3):711–8. https://doi.org/10.1002/bit.21459.
17. Chandran PL, Paik DC, Holmes JW. Structural mechanism for alteration of collagen gel mechanics by glutaraldehyde crosslinking. Connect Tissue Res. 2012;53(4):285–97. https://doi.org/10.3109/03008207.2011.640760. PubMed PMID: WOS:000306190400002.
18. Blauer G, Zvilichovsky B, Yanai P, Meir E, Swenson MK. The interaction of glutaraldehyde with poly(α,L-lysine), n-butylamine, and collagen. II. Hydrodynamic, electron microscopic, and optical investigations on the reaction products. Biopolymers. 1975;14(12):2599–612. https://doi.org/10.1002/bip.1975.360141215.
19. Singh RS, Singh T. Glutaraldehyde functionalization of halloysite nanoclay enhances immobilization efficacy of endoinulinase for fructooligosaccharides production from inulin. Food Chem. 2022;381:132253. https://doi.org/10.1016/j.foodchem.2022.132253.
20. Liu YS, Jiang JZ. Preparation of β-ionone microcapsules by gelatin/pectin complex coacervation. Carbohydr Polym. 2023;312:120839. https://doi.org/10.1016/j.carbpol.2023.120839. PubMed PMID: WOS:000968381600001.
21. Khan S, Anwar N. Gelatin/carboxymethyl cellulose based stimuli-responsive hydrogels for controlled delivery of 5-fluorouracil, development, in vitro characterization, in vivo safety and bioavailability evaluation. Carbohydr Polym. 2021;257:117617. https://doi.org/10.1016/j.carbpol.2021.117617. PubMed PMID: WOS:000617786800002.
22. Jones GJ. Letter: Polymerization of glutaraldehyde at fixative pH. J Histochem Cytochem. 1974;22(9):911–3. https://doi.org/10.1177/22.9.911. PubMed PMID: MEDLINE:4213220.
23. Xu J, Liu F, Wang T, Goff HD, Zhong F. Fabrication of films with tailored properties by regulating the swelling of collagen fiber through pH adjustment. Food Hydrocoll. 2020;108:106016. https://doi.org/10.1016/j.foodhyd.2020.106016.
24. Farris S, Song JH, Huang QR. Alternative reaction mechanism for the cross-linking of gelatin with glutaraldehyde. J Agric Food Chem. 2010;58(2):998–1003. https://doi.org/10.1021/jf9031603. PubMed PMID: WOS:000273671900045.
25. Wang P, Zou Y, Li Y, Qin Z, Liu X, Zhang H. pH-sensitive self-assembled nanofibers based on electrostatic interaction and Schiff base bonding for controlled release of curcumin. Food Hydrocoll. 2022;131:107805. https://doi.org/10.1016/j.foodhyd.2022.107805.
26. Lin J, Pan D, Sun Y, Ou C, Wang Y, Cao J. The modification of gelatin films: based on various cross-linking mechanism of glutaraldehyde at acidic and alkaline conditions. Food Sci Nutr. 2019;7(12):4140–6. https://doi.org/10.1002/fsn3.1282. PubMed PMID: WOS:000501181100001.
27. Akbar I, Jaswir I, Jamal P. Optimisation of the production of fish gelatine nanoparticles as a carrier for sunflower-derived biopeptide. Int Food Res J. 2020;27(1):171–81. PubMed PMID: WOS:000538056000018.
28. Slusarewicz P, Zhu K, Hedman T. Kinetic characterization and comparison of various protein crosslinking reagents for matrix modification. J Mater Sci Mater Med. 2010;21(4):1175–81. https://doi.org/10.1007/s10856-010-3986-8.
29. Mauri AN, Añón MC. Effect of solution pH on solubility and some structural properties of soybean protein isolate films. J Sci Food Agric. 2006;86(7):1064–72. https://doi.org/10.1002/jsfa.2457.
30. Kawahara J-I, Ishikawa K, Uchimaru T, Takaya H. Chemical cross-linking by glutaraldehyde between amino groups: its mechanism and effects. Polym Modif. 1997:119–31. https://doi.org/10.1007/978-1-4899-1477-4_11.
31. Kawahara J, Ohmori T, Ohkubo T, Hattori S, Kawamura M. The structure of glutaraldehyde in aqueous solution determined by ultraviolet absorption and light scattering. Anal Biochem. 1992;201(1):94–8. https://doi.org/10.1016/0003-2697(92)90178-a.
32. Zuo P, Zhang J, Zhou Y, Xie N, Xiao D. Spontaneous formation of fluorescent carbon nanoparticles in glutaraldehyde solution and their fluorescence mechanism. J Fluoresc. 2021;31(2):509–16. https://doi.org/10.1007/s10895-020-02678-w.
33. Zhang T, Yu Z, Ma Y, Chiou BS, Liu F, Zhong F. Modulating physicochemical properties of collagen films by cross-linking with glutaraldehyde at varied pH values. Food Hydrocoll. 2022;124:107270. https://doi.org/10.1016/j.foodhyd.2021.107270. PubMed PMID: WOS:000708639600005.
34. Chen C, Liu F, Yu Z, Ma Y, Goff HD, Zhong F. Improvement in physicochemical properties of collagen casings by glutaraldehyde cross-linking and drying temperature regulating. Food Chem. 2020;318:126404. https://doi.org/10.1016/j.foodchem.2020.126404. PubMed PMID: WOS:000520858000034.
35. He L, Lan W, Cen L, Chen S, Liu S, Liu Y, et al. Improving catalase stability by its immobilization on grass carp (Ctenopharyngodon idella) scale collagen self-assembly films. Mater Sci Eng C. 2019;105:110024. https://doi.org/10.1016/j.msec.2019.110024.
36. Sun L, Li B, Song W, Si L, Hou H. Characterization of Pacific cod (Gadus macrocephalus) skin collagen and fabrication of collagen sponge as a good biocompatible biomedical material. Process Biochem. 2017;63:229–35. https://doi.org/10.1016/j.procbio.2017.08.003.

37. Yan M, Li B, Zhao X, Qin S. Effect of concentration, pH and ionic strength on the kinetic self-assembly of acid-soluble collagen from walleye pollock (Theragra chalcogramma) skin. Food Hydrocoll. 2012;29(1):199–204. https://doi.org/10.1016/j.foodhyd.2012.02.014.
38. Zhang Y, Ingham B, Leveneur J, Cheong S, Yao Y, Clarke DJ, et al. Can sodium silicates affect collagen structure during tanning? Insights from small angle X-ray scattering (SAXS) studies. RSC Adv. 2017;7(19):11665–71. https://doi.org/10.1039/c7ra01160a.
39. Liao J, Yang L, Grashow J, Sacks MS. Molecular orientation of collagen in intact planar connective tissues under biaxial stretch. Acta Biomater. 2005;1(1):45–54. https://doi.org/10.1016/j.actbio.2004.09.007.
40. Miao KY, Li XY, Yang D, Xu YB, Mu CD, Li DF, et al. Hydrothermal shrinkage behavior of pigskin. Thermochim Acta. 2021;699:178896. https://doi.org/10.1016/j.tca.2021.178896. PubMed PMID: WOS:000659820000007.
41. Aktaş N. The effects of pH, NaCl and $CaCl_2$ on thermal denaturation characteristics of intramuscular connective tissue. Thermochim Acta. 2003;407(1–2):105. https://doi.org/10.1016/s0040-6031(03)00306-x.
42. Shi R, He J, Jirimutu. Ultrasonic-assisted extraction and structure characterization of collagen from camel skin. J Chin Inst Food Sci Technol. 2022;22(2):213–23. https://doi.org/10.16429/j.1009-7848.2022.02.023. (in Chinese).
43. Wang Y-N, Hu L. Essential role of isoelectric point of skin/leather in leather processing. J Leather Sci Eng. 2022;4:25. https://doi.org/10.1186/s42825-022-00099-y.
44. Gray RE, Seng N, Mackay IR, Rowley MJ. Measurement of antibodies to collagen II by inhibition of collagen fibril formation in vitro. J Immunol Methods. 2004;285(1):55–61. https://doi.org/10.1016/j.jim.2003.11.010.
45. Jingmin W, Fei L, Zhe Y, Yun M, Douglas GH, Jianguo M, et al. Facile preparation of collagen fiber-glycerol-carboxymethyl cellulose composite film by immersing method. Carbohydr Polym. 2020;229:115429. https://doi.org/10.1016/j.carbpol.2019.115429.
46. Nilsuwan K, Fusang K, Pripatnanont P, Benjakul S. Properties and characteristics of acid-soluble collagen from salmon skin defatted with the aid of ultrasonication. Fishes (MDPI AG). 2022;7(1):51. https://doi.org/10.3390/fishes7010051.
47. Zhang Y, Snow T, Smith AJ, Holmes G, Prabakar S. A guide to high-efficiency chromium (III)-collagen cross-linking: synchrotron SAXS and DSC study. Int J Biol Macromol. 2019;126:123–9. https://doi.org/10.1016/j.ijbiomac.2018.12.187.
48. Sizeland KH, Edmonds RL, Basil-Jones MM, Kirby N, Hawley A, Mudie S, et al. Changes to collagen structure during leather processing. J Agric Food Chem. 2015;63(9):2499–505. https://doi.org/10.1021/jf506357j.
49. Gillett R, Gull K. Glutaraldehyde–its purity and stability. Histochemie. 1972;30(2):162–7. https://doi.org/10.1007/bf01444063.
50. Cheung DT, Nimni ME. Mechanism of crosslinking of proteins by glutaraldehyde I: reaction with model compounds. Connect Tissue Res. 2009;10(2):187–99. https://doi.org/10.3109/03008208209034418.
51. Ruijgrok JM, Boon ME, Wijn JRD. The effect of heating by microwave irradiation and by conventional heating on the aldehyde concentration in aqueous glutaraldehyde solutions. Histochem J. 1990;22(6–7):389–93. https://doi.org/10.1007/bf01003175.

Publisher's Note